Electronic Supplementary Information

Multifunctional Anode Materials with P-Doped Si Nanoparticles in Conductive and Stress-Buffering Network of Poly-γ-Polyglutamate and Graphene

*Ren Na [#, †], Nadine Madiou[#], Ning Kang[#], Shan Yan[#], Jin Luo[#], Guojun Liu, Zhongqiang Shan, Jianhua Tian[†, *], Chuan-Jian Zhong[#,*]*

Dr. Ren Na, Nadine Madiou, Dr. Ning Kang, Dr. Shan Yan, Dr. Jin Luo, Prof. Chuan-Jian Zhong
Department of Chemistry, State University of New York at Binghamton, Binghamton, New York 13902, United States
E-mail: cjzhong@binghamton.edu

Dr. Ren Na, Prof. Jianhua Tian and Prof. Zhongqiang Shan
School of Chemical Engineering and Technology, Tianjin University, Tianjin, 300350, China
E-mail: jhtian@tju.edu.cn

Dr. Guojun Liu
Suzhou Gorichen Technology Co., Suzhou Wuzhong Economic Development Zone, China

Experimental Section

Chemmicals

Graphite flake (~325 mesh, 99.8%) and hydrogen peroxide (30%) were purchased from Alfa Aesar. Sulfuric Acid (98%) and phosphoric acid (86%) were purchased from J.T.Baker. Potassium permanganate (99%) and L-Ascorbic Acid (99%) were bought from Sigma Aldrich. The deionized water (18.2 M Ω) obtained by the purification system was used. All the chemicals were used as received.

Synthesis of P-Si/G

Graphene oxide was prepared by modified Hummer's method reported previous work. P-Si nanoparticles were synthesized via spark-discharge method by using SiH_4 and PH_3 and the final P content in P-Si is around 20 ppm which is identified by XRF and the average size of P-Si is 110 nm. Generally, 100 mg of P-Si nanoparticles were dispersed into 100 mL of graphene oxide aqueous solution with a concentration of 0.2 mg mL^{-1} under ultrasonic for 0.5 h. Subsequently, 20 mg of L-ascrobic as the reductant was added into above mixture and the temperature of the reaction system was heated at 75 °C for 8 h. The intermediate was washed by water and ethanol, finally dried in vacuum oven under 60 °C overnight followed by annealing under argon atmosphere at 550 °C for 2 h. For comparison, we also synthesized P-

Si/C composite using commercial carbon material, i.e. graphene nanoplates (GNPs) and carbon nanotube (CNT). With the same loading of P-Si, P-Si/C composites were obtained by sonication with the above carbon materials aqueous solutions and following stirring overnight. The corresponding P-Si/C composites are denoted as P-Si/GNPs and P-Si/CNT.

Synthesis of different cations modified PGA

PGA was synthesized according to previous work. Different cations modified PGA were obtained by adding PGA powder directly into 0.1 M LiOH, NaOH, KOH and ammonia under magnetic stirring for 12 h and the pH value of the mixture was fixed at 9. The above solution were used as binder directly.

Materials Characterization

The morphology and inner structure of P-Si/G were characterized by scanning electron microscope (SEM, LEO-1550), transmission electron microscopy (TEM, JEOL JEM-ARM200F) and X-ray diffraction (XRD). Thermogravimetric analysis (TGA) was performed from room temperature to 900 °C under air atmosphere. The fourier transform infrared spectroscopy (FT-IR) spectra of Nano-Si were documented with KBr pellets from Avatar360 (Thermo Nicolet, USA). The viscosity test was conducted at room temperature by using a cone-plate rheometer (AR1000, Texas Instrument).

Electrochemical performance tests were done using CR2032-type coin cell with a MPG2 potential station (EC lab software, BioLogic) in a potential voltage from 0.01 to 1 V vs Li^+/Li at room temperature. The working electrodes were composed of P-Si/G composite (80 wt%), Super P (10 wt%) and alginate sodium or PGA which was synthesized by our previous study (10 wt %). The mass loading of P-Si/G electrode is from 0.9~1.2 mg cm^{-2}. Lithium foil was used as counter electrode and the separator is from Celgard C480. The electrolyte solution was 1M $LiPF_6$/ethylene carbonate (EC)/dimethyl carbonate (DMC) (1:1 by volume). The batteries were assembled in glove box with oxygen and water content less than 0.1 ppm.

The morphology of the P-Si/G electrode before and after 1 cycle is characterized by optical microscopy (Nikon, ECLIPSE).

Additional Figures and Table:

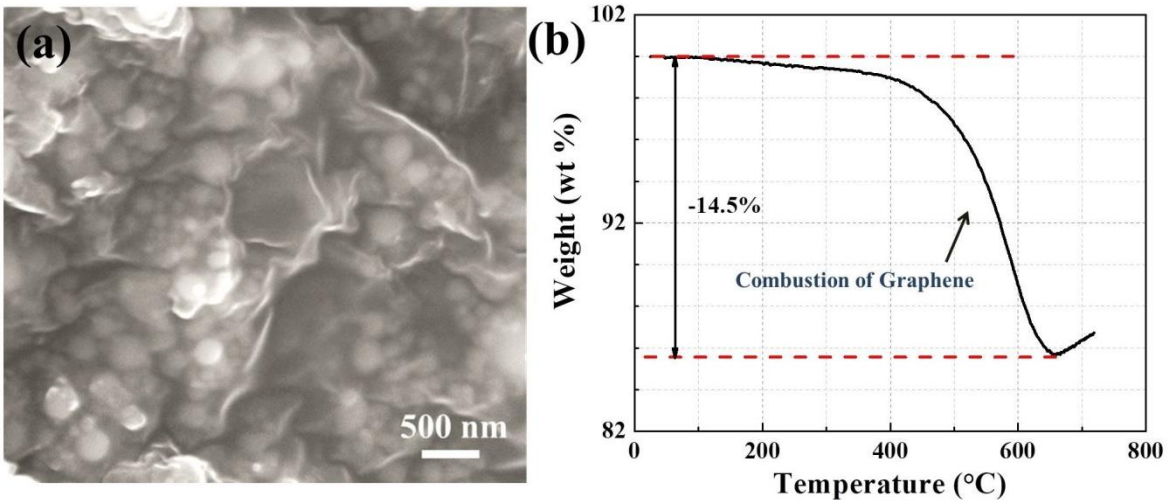

Figure S1. SEM (a) and TGA curve (b) of P-Si/G composite.

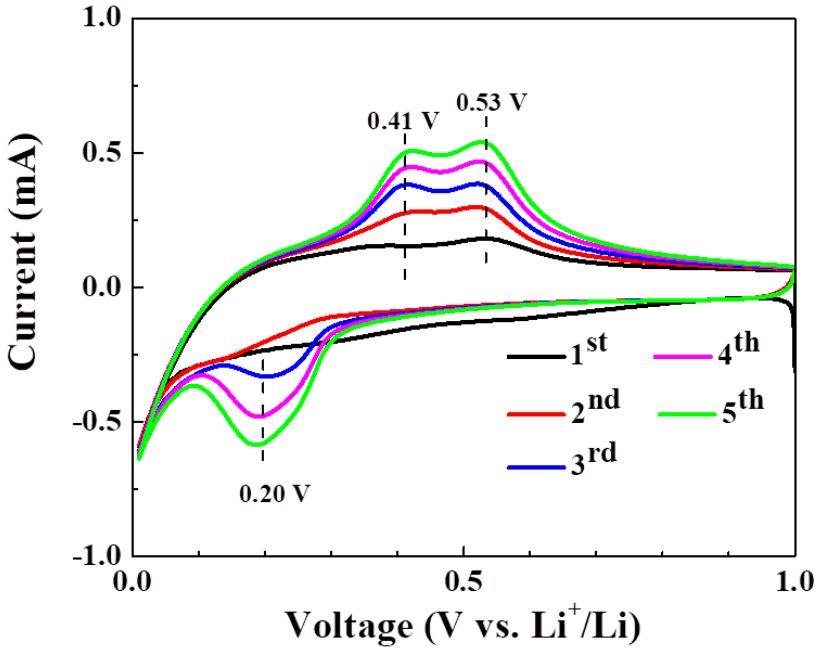

Figure S2 Cyclic voltammetric curves showing the electrochemical performance of the P-Si/G composite.

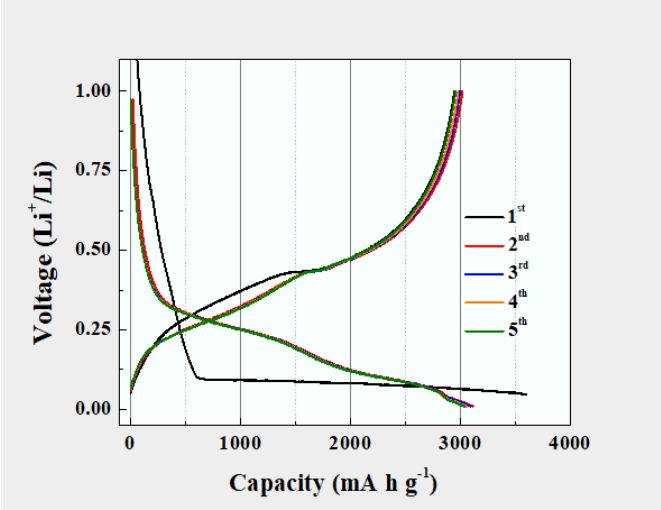

Figure S3. Charge/discharge curve of P-Si/G electrode.

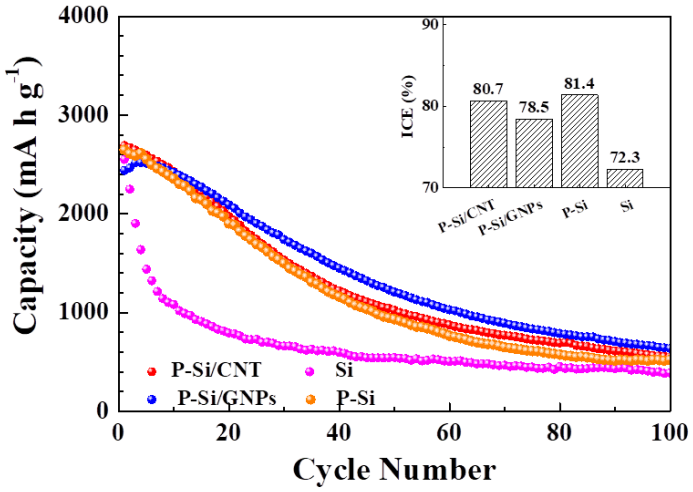

Figure S4. Cycling performance of P-Si/CNT, P-Si/GNPs, P-Si and Si electrode.

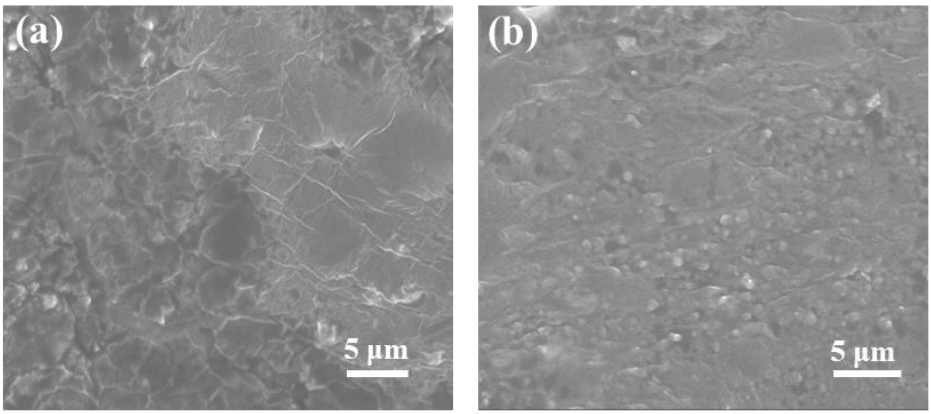

Figure S5. Comparison of morphology between Si electrode (a) and P-Si/G (b) electrode after cycling.

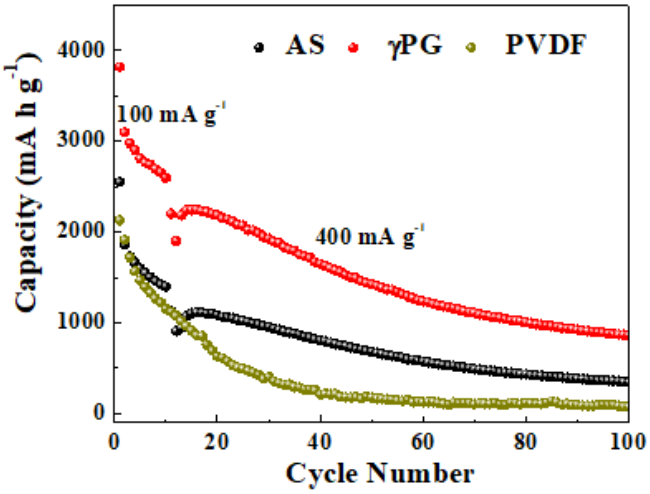

Figure S6. Cycling performance of Si nanoparticles electrode by utilizing different binders.

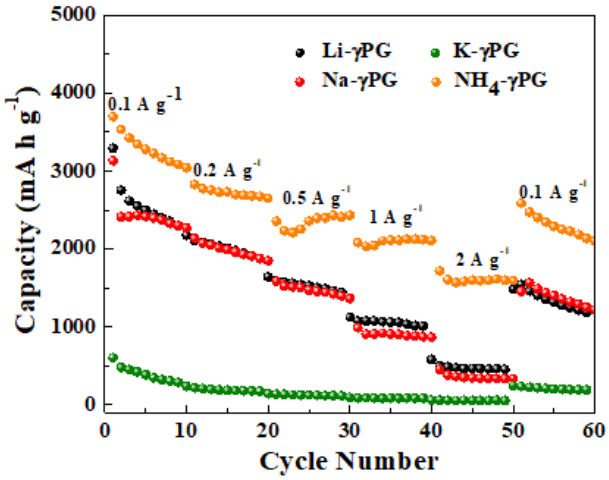

Figure S7. Rate capability of Si nanoparticles electrode using different cations modified PGA.

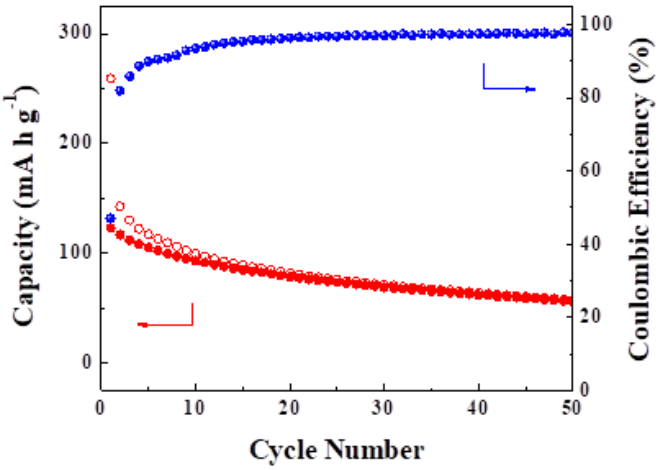

Figure S8. Cycling performance of P-Si/G electrode full cell using LCO as cathode at 1 C between 2 and 4.3 V.

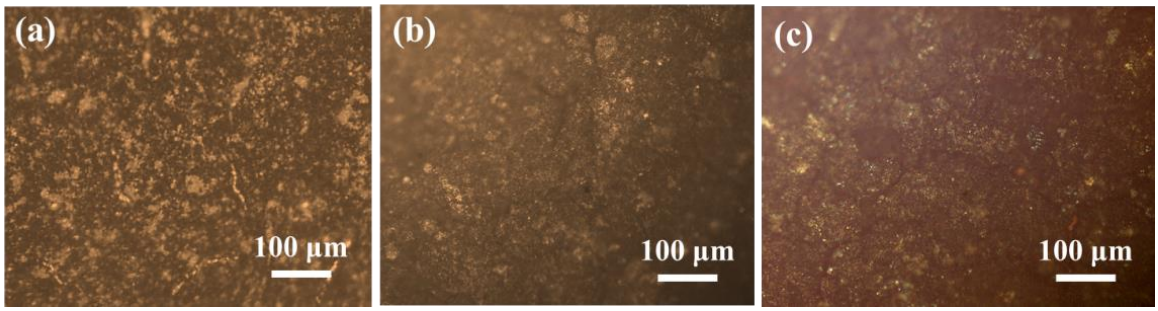

Figure S9. Direct observing of self-healing capability of P-Si/G electrode: (a) before cycling, (b) after 1st discharge and (c) after 1st discharge for 5 min.

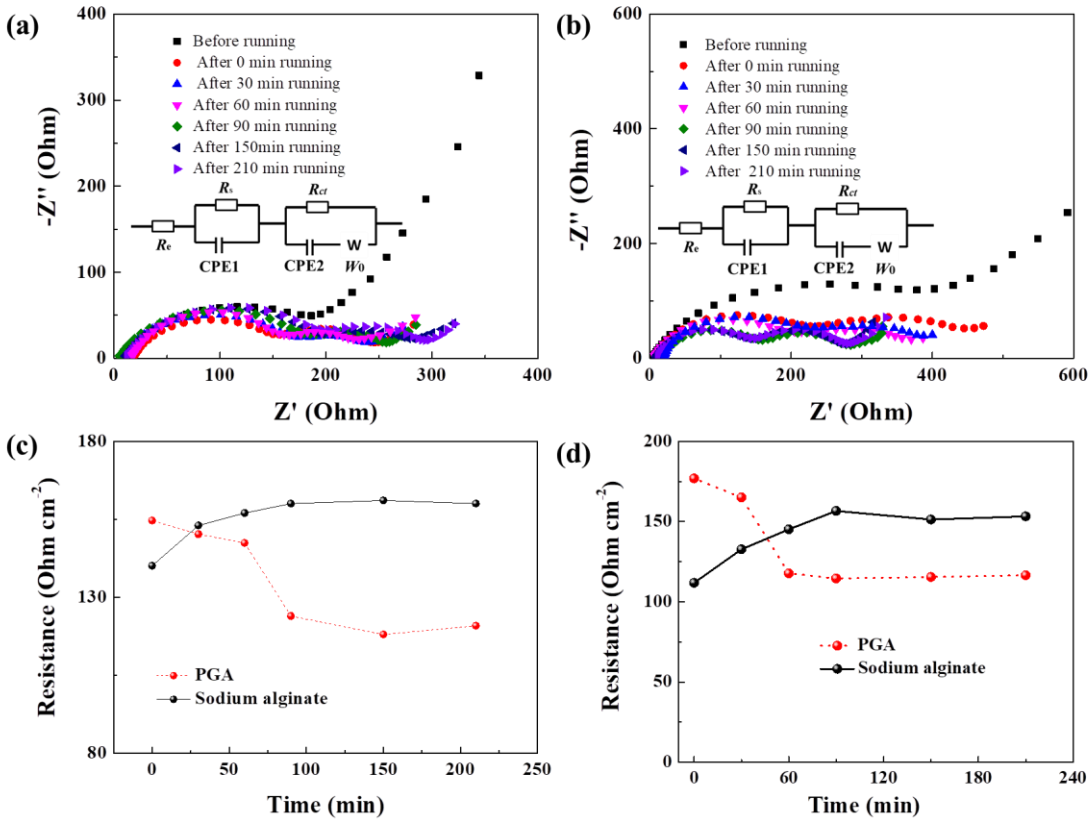

Figure S10. Time-dependent Nyquist plot of P-Si/G electrode using sodium alginate (a) and PGA (b) as binder. (inset is the equivalent circuit), the R_{SEI} and R_{ct} values of P-Si/G electrode with PGA and sodium alginate binder changes along with the time (c) and (d).

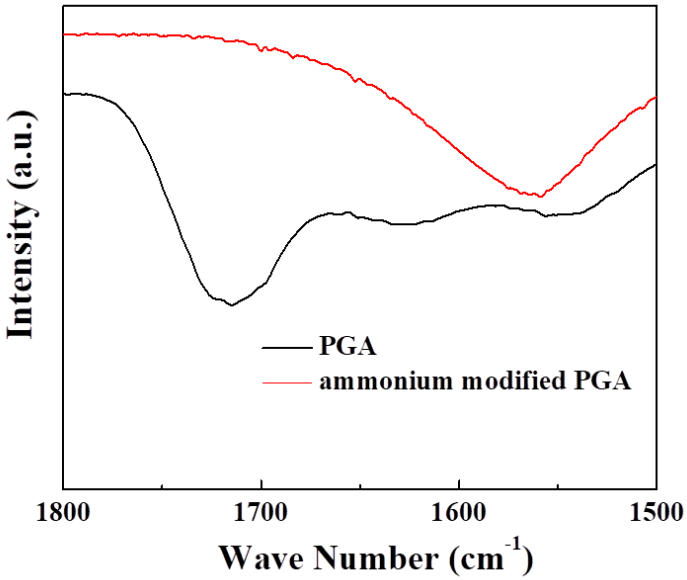

Figure S11. FTIR spectra of PGA and ammonia modified PGA.

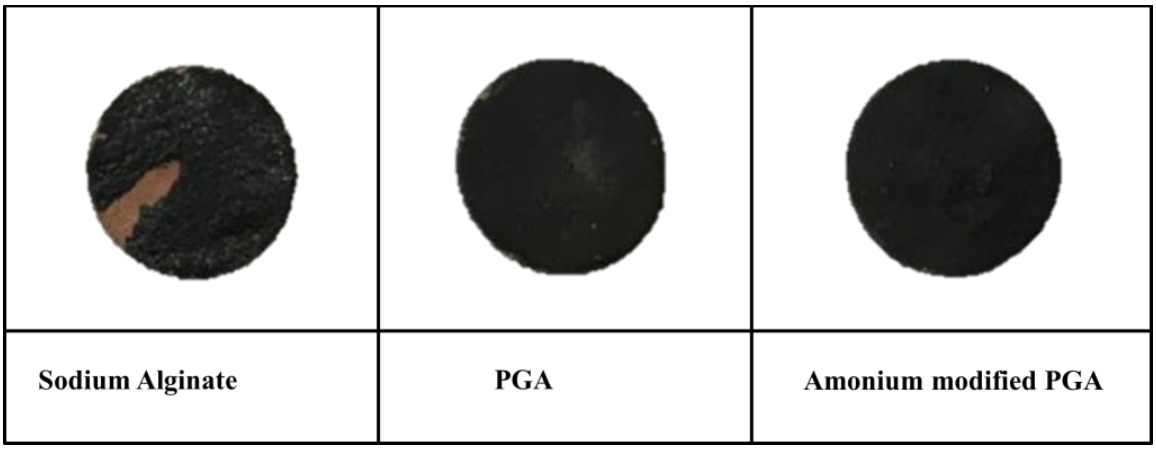

Figure S12. Digital graph of P-Si electrodes after 100 cycles using sodium alginate, PGA and amonium modified PGA as binder.

Table S1. Viscosity of Li^+, Na^+, K^+ and NH_4^+ modified PGA solution (at 25 ℃ when the concentration is 0.6 mg mL^{-1}).

	Li-γPGA	**Na-γPGA**	**K-γPGA**	**NH_4-γPGA**	**γPGA**	**DI water**
Viscosity (mPa▪s)	2.6	2.6	2.7	3.7	2.8	0.9

Table S2. Comparision of mass loading and electrochemical performance of previous reported Si anode.

Ref.	Mass loading (mg cm^{-2})	Cycling performance
[1]	1	722mAh g^{-1} at 0.1 A g^{-1} after 100 cycles
[2]	0.9	1325 mAh g^{-1} at 0.2 A g^{-1} after 60 cycles
[3]	1	1660 mAh g^{-1} at 0.2 A g^{-1} after 100 cycles
[4]	1.5	534.3 mAh g^{-1} at 0.5 A g^{-1} after 200 cycles
[5]	0.8-1.2	1107 mAh g^{-1} at 0.5 A g^{-1} after 100 cycles
[6]	0.6-0.7	1000 mAh g^{-1} at 0.1 A g^{-1} after 50 cycles
[7]	1.4	595 mAh g^{-1} at 0.2 A g^{-1} after 200 cycles
[8]	0.8-1.1	1002 mAh g^{-1} at 0.1 A g^{-1} after 100 cycles
[9]	0.7	1670 mAh g^{-1} at 0.1 C after 100 cycles
[10]	0.8-1	1031 mAh g^{-1} at 0.5 A g^{-1} after 100 cycles
[11]	0.5-0.7	1300 mAh g^{-1} at 0.5C after 150 cycles

References

[1] Sun Y, Lopez J, Lee H-W, et al. A Stretchable Graphitic Carbon/Si Anode Enabled by Conformal Coating of a Self-Healing Elastic Polymer[J]. Advanced Materials, 2016, 28(12): 2455-2461.

[2] Liang G, Qin X, Zou J, et al. Electrosprayed silicon-embedded porous carbon microspheres as lithium-ion battery anodes with exceptional rate capacities[J]. Carbon, 2018, 127: 424-431.

[3] Yi Z, Qian Y, Cao C, et al. Porous Si/C microspheres decorated with stable outer carbon interphase and inner interpenetrated Si@C channel for enhanced lithium storage[J]. Carbon, 2019, 149: 664-671.

[4] Cui M, Wang L, Guo X, et al. Designing of hierarchical mesoporous/macroporous silicon-based composite anode material for low-cost high-performance lithium-ion batteries[J]. Journal of Materials Chemistry A, 2019, 7(8): 3874-3881.

[5] Liu N, Liu J, Jia D, et al. Multi-core yolk-shell like mesoporous double carbon-coated silicon nanoparticles as anode materials for lithium-ion batteries[J]. Energy Storage Materials, 2019, 18: 165-173.

[6] Wang K-L, Kuo T-H, Yao C-F, et al. Cyclopentadithiophene-benzoic acid copolymers as conductive binders for silicon nanoparticles in anode electrodes of lithium ion batteries[J]. Chemical Communications, 2017, 53(11): 1856-1859.

[7] Parekh M H, Parikh V P, Kim P J, et al. Encapsulation and networking of silicon nanoparticles using amorphous carbon and graphite for high performance Li-ion batteries[J]. Carbon, 2019, 148: 36-43.

[8] Zhang F, Zhu G, Wang K, et al. Encapsulation of core–satellite silicon in carbon for rational balance of the void space and capacity[J]. Chemical Communications, 2019, 55(71): 10531-10534.

[9] Shin J, Cho E. Agglomeration Mechanism and a Protective Role of Al_2O_3 for Prolonged Cycle Life of Si Anode in Lithium-Ion Batteries[J]. Chemistry of Materials, 2018, 30(10): 3233-3243.

[10] Zhang Y-C, You Y, Xin S, et al. Rice husk-derived hierarchical silicon/nitrogen-doped carbon/carbon nanotube spheres as low-cost and high-capacity anodes for lithium-ion batteries[J]. Nano Energy, 2016, 25: 120-127.

[11] Munaoka T, Yan X, Lopez J, et al. Ionically Conductive Self-Healing Binder for Low Cost Si Microparticles Anodes in Li-Ion Batteries[J]. Advanced Energy Materials, 2018, 8(14): 1703138.